Supporting Information

Photostable Ratiometric Pdot Probe for in Vitro and in Vivo Imaging of Hypochlorous Acid

Li Wu,[†] I-Che Wu,[†] Christopher C. DuFort,[‡] Markus A. Carlson,[‡] Xu Wu,[†] Lei Chen,[†] Chun-Ting Kuo,[†] Yuling Qin,[†] Jiangbo Yu,[†] Sunil R. Hingorani,[‡,§,⊥] and Daniel T. Chiu*[†]

[†]Department of Chemistry, University of Washington, Seattle, Washington 98195, United States

[‡]Clinical Research Division and [§]Public Health Sciences Division, Fred Hutchinson Cancer Research Center, Seattle, Washington 98109, United States

[⊥]Division of Medical Oncology, University of Washington School of Medicine, Seattle, Washington 98195, United States

*Email: chiu@chem.washington.edu

Experimental Section:

1. Materials

Fluorescein, sodium hypochlorite solution, hydrogen peroxide solution (30%), potassium dioxide (KO_2), phorbol 12-myristate 13-acetate (PMA), lipopolysaccharide (LPS), N-acetyl-L-cysteine (NAC), 4-aminobenzioc hydrazide (ABAH), 1,4-dithiothreitol (DTT), L-glutathione reduced (GSH), L-cysteine (Cys), DL-homocysteine (Hcy), 3-(4,5-dimethylthiahiazol-2-y1)-2,5-diphenyl tetrazolium bromide (MTT assay kit), and Luperox® TBH70X, tert-butyl hydroperoxide solution (t-BuOOH) were purchased from Sigma Aldrich (St. Louis, MO, USA). Angeli's salt and peroxynitrite were obtained from Cayman Chemical Company (Michigan, USA). Polystyrene graft ethylene oxide functionalized with carboxyl groups (PS-PEG-COOH; MW 21 700 Da of PS moiety; 1200 Da of PEG-COOH; polydispersity, 1.25) was from Polymer Source Inc. (Quebec, Canada). Eagle's minimum essential medium (EMEM), Dulbecco's Modified Eagle's Medium (DMEM), fetal bovine serum (FBS), penicillin and streptomycin were obtained from the American Type Culture Collection (ATCC). All reagents were of analytical grade, and used as received. All aqueous solutions were prepared with nanopure water (18.2 MΩ cm, Milli-Q, Millipore).

2. Apparatus and characterizations

^1H (500 MHz) and ^{13}C (125 MHz) NMR spectra were recorded on Bruker AV500 spectrometers. ^1H

NMR and ^{13}C NMR spectra used tetramethylsilane (TMS) as an internal standard in $CDCl_3$. The molecular weight of polymers was measured by the GPC method (Viscotek TDA305 GPC), where polystyrene was used as the standard (THF as eluent). ESI-MS spectra were obtained using a Bruker APEX Qe 47e Fourier transform (ion cyclotron resonance) mass spectrometer. The size of Pdots in bulk solution was characterized by dynamic light scattering using Malvern Zetasizer NanoS. Transmission electron microscopic (TEM) images were recorded using FEI Tecnai F20 high-resolution transmission electron microscope operating at 200 kV. The UV-vis measurements of Pdots were performed on a DU 720 scanning spectrophotometer (Beckman Coulter, Inc., CA USA). All the fluorescence spectra were carried out on a commercial Fluorolog-3 fluorometer (HORIBA Jobin Yvon, NJ USA) equipped with a temperature-controlled water bath. Fluorescence quantum yields were measured using a Hamamatsu photonic multichannel analyzer C10027 equipped with a CCD camera and an integrating sphere. For the quantum-yield calibration, we used the solvent as the reference. The fluorescence images of stained cells were acquired with a fluorescence confocal microscope (Zeiss LSM 510); the excitation wavelength was 405 nm. Fluorescence images of 96-well microplates and animals were taken with IVIS Spectrum In Vivo Imaging System (Perkin Elmer). Flow cytometry experiments were performed on a BD LSR II Special Order System; the excitation wavelength was 405 nm. All the experiments were carried out at room temperature, unless otherwise specified.

3. Synthesis of $PFOBT_{36}SeTBT_x$ polymers[1]

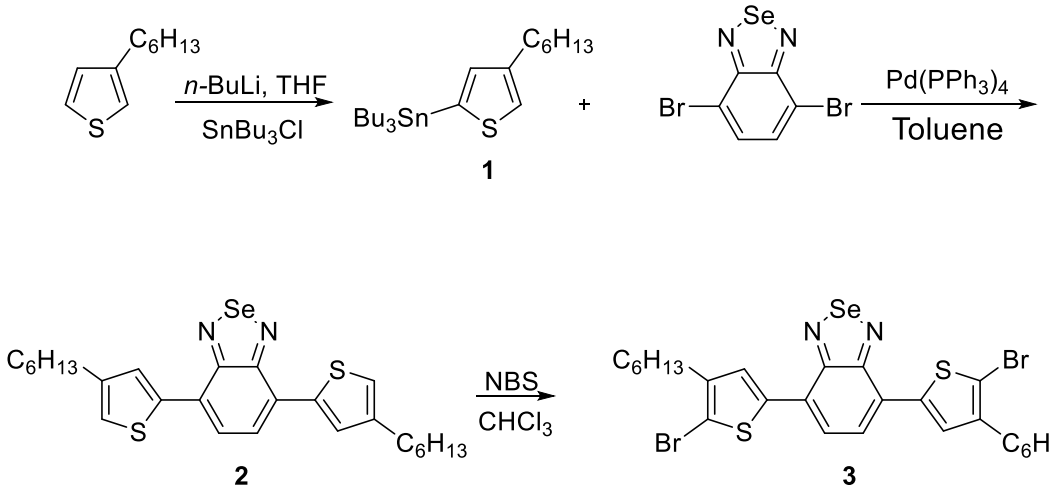

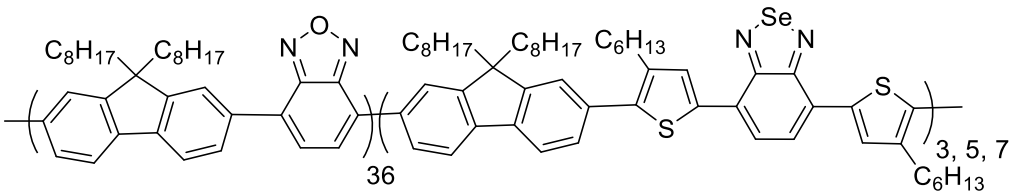

Synthesis of compound 1: tributyl(4-hexylthiophen-2-yl)stannane

3-hexylthiophene (936 mg, 5.65 mmol) was dissolved in 20-mL dry THF and then cooled to -78 °C. Then 2.5 M *n*-BuLi (2.7 mL, 6.72 mmol) was added dropwise to the reaction. The reaction was warmed up to room temperature and stirred for 2 hours and cooled to 0 °C, then 5.9 mL of Me_3SnCl was added and reacted for 2 hours. The reaction was poured into water and extracted with ether, washed by brine and dried in the vacuum. The final product was obtained at 2.31 g (91%).

^{1}H NMR (500 MHz, ($CDCl_3$) = 7.20 (s, 1H), 7.01(s, 1H), 2.65 (t, 2H), 1.65~1.55 (m, 4H), 1.37~1.29 (m, 12H), 1.48~1.24 (m, 26H), 0.90~0.88 (m, 4H), 0.41~0.30 (m, 12H). HR-MS (*m/z,* ESI): (M^+, $C_{22}H_{42}SSn$) calculated *m/z* = 458.2029; found *m/z* = 458.32027.

Synthesis of compound 2: 4,7-bis(4-hexylthiophen-2-yl)benzo[c][1,2,5]selenadiazole

4,7-dibromobenzo[c] [1,2,5]selenadiazole (778 mg, 2.31 mmol) and tributyl(4-hexylthiophen-2-yl)stannane (1760 mg, 5.32 mmol) were dissolved in dry THF and degassed at -78 °C three times. Then, $Pd(PPh_3)_4$ (160 mg, 0.14 mmol) was added and refluxed in 120 °C for 24 h. Finally, we removed the solvent. The product was purified by column chromatography with silica gel to yield 536 mg (45%) of product.

^{1}H NMR (500 MHz, ($CDCl_3$) = 7.87 (s, 2H), 7.74 (s, 1H), 7.04(s, 1H), 2.69 (t, 4H), 1.69~1.67 (m, 4H), 1.55~1.31 (m, 12H), 0.90 (t, 6H). ^{13}C NMR (300 MHz, $CDCl_3$) =157.8, 142.6, 138.8, 127.7, 126.8, 124.9, 112.2, 31.6, 29.7, 28.9, 22.6, 14.0. HR-MS (*m/z,* ESI): (M^+, $C_{26}H_{32}N_2S_2Se$) calculated *m/z* = 516.1172; found *m/z* = 516.1172.

Synthesis of compound 3: 4,7-bis(5-bromo-4-hexylthiophen-2-yl)benzo[c][1,2,5]selenadiazole

4,7-bis(4-hexylthiophen-2-yl) benzo[c][1,2,5]selenadiazole (958 mg, 1.86 mmol) was dissolved in 30 mL of DMF. NBS was added (684 mg, 3.84 mmol) into reaction. After reacting at room temperature for 11 h, the solution was poured into water and extracted with CH_2Cl_2 and brine. The solvent was removed and the product was purified by column chromatography to get 1064 mg (85%) of product.

^{1}H NMR (500 MHz, ($CDCl_3$) = 7.69 (s, 2H), 7.66 (s, H), 2.63 (t, 4H), 1.68~1.61 (m, 4H),

1.42~1.35(m, 12H), 0.90 (t, 6H). ^{13}C NMR (300 MHz, $CDCl_3$) = 158.3, 144.0, 139.4, 129.0, 127.6, 125.8, 121.8, 31.7, 30.7, 30.5, 29.0, 22.6, 14.0.

The general procedure for the preparation of polymer ($PFOBT_{36}SeTBT_x$)

The polymer was synthesized by different feeding ratios of monomer into the Suzuki coupling reaction.

$PFOBT_{36}SeTBT_3$

9, 9-Dioctylfluorene-2, 7-diboronic acid bis(1, 3-propanediol)ether (56 mg, 0.1 mmol), 9, 9-Dioctyl-2, 7-dibromofluorene (12 mg, 0.022 mmol), 4,7-dibromobenzo[c][1,2,5]oxadiazole (20 mg, 0.072 mmol), 4,7-bis(5-bromo-4-hexylthiophen-2-yl)benzo[c][1,2,5]selenadiazole (4 mg, 0.006 mmol), 20% Et_4NOH (3mL), and $Pd(PPh_3)_4$ (4 mg, 3 mol%) was added in toluene (7 mL) . The mixture was degassed, refilled with N_2 and refluxed for 2 days. Phenylboronic acid (20 mg), dissolved in THF (0.5 mL), was added to the reaction. After 2 hours' reaction, bromobenzene (0.5 mL) was added and further stirred for 3 hours. The mixture was poured into methanol (100 mL) and the precipitate was filtered, washed with methanol, water and acetone to remove any monomers, small oligomers and inorganic salts. The crude product was dissolved in DCM (7 mL), filtered through a 0.2-μm membrane and re-precipitated in methanol (75 mL). The powder was then dissolved and stirred in acetone (100 mL) for 4 hours and collected by filtration and dried in vacuum. (Yield: 75%) *Mn* = 19600, PDI = 2.8

$PFOBT_{36}SeTBT_5$ *Mn* = 10400, PDI = 3.8

$PFOBT_{36}SeTBT_7$ *Mn* = 16100, PDI = 2.9

4. Preparations of $PFOBT_{36}SeTBTx$ Pdots

$PFOBT_{36}SeTBTx$ Pdots were prepared by the nanoprecipitation method as described in our previous report.[2,3] Briefly, the fluorescent semiconducting polymer $PFOBT_{36}SeTBTx$ was first dissolved in THF to produce a 1 mg/mL stock solution. Then, the stock $PFOBT_{36}SeTBTx$ solution was diluted in THF with 20 μg/mL copolymer PS-PEG-COOH to make a solution mixture with the final $PFOBT_{36}SeTBTx$ concentration of 100 μg/mL. The mixture was sonicated in an ice-water bath to form a homogeneous solution. A 5-mL aliquot of the solution mixture was quickly injected into 10 mL of Milli-Q water under vigorous sonication in an ice-bath ultrasonicator. THF was removed by blowing nitrogen gas into the solution on a 100 °C hot plate for about 1h. The resulting Pdot solution

was sonicated for 1-2 minutes and filtered through a 0.2-μm cellulose membrane filter to remove any aggregates before use.

5. Generation of Different ROS/RNS

ClO^- was prepared by directly diluting commercially available NaClO and the concentration was determined from absorption at λ=292 nm (ε = 350 $M^{-1}\cdot cm^{-1}$). H_2O_2 stock solution was prepared by diluting 30% H_2O_2 solution, and the concentration was determined from absorption at λ=240 nm (ε=43.6 $M^{-1}\cdot cm^{-1}$). $O_2^{\cdot-}$ was generated from KO_2 solid diluted in DMSO; the concentration was determined from absorption at λ=550 nm (ε = 21.6 $mM^{-1}\cdot cm^{-1}$). t-BuOO was generated by reaction between $FeSO_4$ and t-BuOOH, and concentration of t-BuOO·was determined by Fe^{2+}. $ONOO^-$ was used from the stock solution in NaOH and the concentration was determined from absorption at λ=302 nm (ε = 1670 $M^{-1}\cdot cm^{-1}$). ·OH was generated by the Fenton reaction between $FeSO_4$ and H_2O_2, and concentration of·OH was determined by Fe^{2+}. Note that Fe^{2+} and Fe^{3+} ions showed no fluorescence quenching of the nanoparticle. Angeli's salt was used as a HNO donor and the concentration of Angeli's salt stock solution was determined by measuring the absorbance at λ=248 nm (ε = 8.3×10^3 $M^{-1}\cdot cm^{-1}$) in 1 mM aqueous NaOH solution. The fluorescence spectra (λ_{ex} = 405 nm) of $PFOBT_{36}SeTBTx$ Pdots (10 μg/mL) in PBS (10 mM, pH = 7.4) were measured 5 min after addition of ROS. PBS used for the experiments was purged with nitrogen for 1 hour before the measurement.

6. Cell culture

The breast cancer line MCF-7 and RAW 264.7 murine macrophage cells were purchased from American Type Culture Collection (Manassas, VA, USA). Primary cultured MCF-7 cells were cultured in EMEM (Eagle's minimum essential medium) culture medium supplemented with 10% FBS, 1% penicillin, and streptomycin. RAW 264.7 cells were cultured in DMEM (Dulbecco's Modified Eagle Medium) supplemented with 10% FBS (fetal bovine serum), 1% penicillin, and streptomycin. All cells were maintained at 37 ºC in a humidified atmosphere (95% air and 5% CO_2).

7. Cytotoxicity test

The toxicity of $PFOBT_{36}SeTBT_5$ Pdots to cells was measured by the MTT assay. Briefly, MCF-7 in

100 μL of EMEM and RAW 264.7 cells in 100 μL DMEM were plated at a density of 1×10^4 cells per well in 96-well plates and kept at 37 °C for 24 h. The cells were exposed to a series of concentrations of Pdots for 24 h, and the viability of the cells was measured using the MTT method. Controls were cultivated under the same conditions without the addition of the nanocomposites. Then, 100 μL of MTT (0.5 mg/mL in EMEM) was added into each well and further incubated for an additional 4 h. Subsequently, the supernatant was discarded, followed by the addition of 100 μL DMSO into each well to dissolve the formed formazan and incubation in the shaker incubator with gentle shakes for 10 min. Then, the optical density (OD) was read at a wavelength of 570 nm. The cell viability rate was expressed as follow: % = [OD] test/[OD] control× 100%. The cell survival rate from the control group was considered to be 100%.

8. Detection of exogenous ClO^- in MCF-7 cells and endogenous ClO^- in RAW 264.7

Cells were collected at the exponential phase of growth. The adherent MCF-7 cells were harvested from the culture flask by quickly rinsing with fresh culture medium followed by digestion with 5 mL of trypsin-EDTA solution (0.25 w/v % trypsin, 2.5 g/L EDTA) at 37 °C for 5 min. After complete detachment, the solution of suspended cells was collected and centrifuged. Then 1×10^5 MCF-7 cells were seeded into a glass-bottomed culture dish and allowed to adhere for 24 h with 10 μg/mL Pdots in a humidified atmosphere of 5% CO_2 and 95% air at 37 °C. Prior to fluorescence imaging, the stained cells were rinsed with PBS solution to remove any nonspecifically absorbed Pdots on cell membrane. For exogenous ClO^- detection, MCF-7 cells loaded with $PFOBT_{36}SeTBT_5$ Pdots were incubated at 37 °C for 30 min in PBS solution (10 mM, pH=7.4) in the presence of different concentration of NaClO. Cells were washed three times with 1×PBS (pH=7.4) buffer prior to imaging. For time-dependent imaging of exogenous ClO^-, MCF-7 cells loaded with $PFOBT_{36}SeTBT_5$ Pdots were treated with 50 μM NaClO. Confocal fluorescence images were recorded at different time points.

For endogenous ClO^- detection in RAW 264.7 cells, the cells were collected at the exponential phase of growth and seeded into glass-bottomed culture dishes. They were allowed to adhere for 24 h in a humidified atmosphere of 5% CO_2 and 95% air at 37 °C. LPS in fresh culture medium at the concentration of 1 μg/mL was added and incubated for 4 h, which was followed by PMA (5 μg/mL) for 0.5 h. Then, cells were cultured with $PFOBT_{36}SeTBT_5$ Pdots (final concentration: 10 μg/mL)

for 4 h. Alternatively, the cells were separately pretreated with free-radical scavenger NAC (1 mM) for 2 h and myeloperoxidase inhibitor ABAH (1 mM) for 2 h before LPS (final concentration: 1 μg/mL) and PMA (final concentration: 5 μg/mL) treatment. Before incubation with $PFOBT_{36}SeTBT_5$ Pdots for 4 h, the cells were treated with NAC (1 mM) and ABAH (1 mM) for 1h. For the control experiment, the cells were only incubated with $PFOBT_{36}SeTBT_5$ Pdots (10 μg/mL) for 4 h. Cells were washed with 1×PBS solution three times before imaging.

Fluorescence imaging experiments were performed on a fluorescence confocal microscope (Zeiss LSM 510) with excitation at 405 nm through 40X/oil objective. Fluorescence emissions were collected through the following two channels of BP 530nm-600nm (BP means "band pass", in which anything between the wavelengths indicated can pass through) and LP 650 nm (LP means "long pass", in which anything longer than the wavelength indicated can pass through) for green and NIR, respectively. Images processing and analysis was carried out on Image J software.

9. Inflammation models

Female nu/nu mice were obtained from Charles River Laboratories International, Inc. (MA, USA). The Institutional Animal Care and Use Committees at the Fred Hutchinson Cancer Research Center approved all the animal studies carried out in this work. The whole animal imaging was performed on a IVIS Spectrum In Vivo Imaging System (Perkin Elmer). Images were acquired with a 0.5-sec acquisition time using an excitation of 465 nm and emission filters of 540 nm and 680 nm. For in vivo imaging of externally added hypochlorite, female nu/nu mouse under anesthesia was given a subcutaneous injection of $PFOBT_{36}SeTBT_5$ Pdots (0.1 mg/mL, 0.1 mL) into the dorsal area. Then, 10 nmol NaClO diluted with 0.1 mL PBS (pH 7.4) solution was injected. For the control experiment, the injection was performed with only PBS solution without NaOCl. At 30 min after injection of NaOCl, fluorescence images were acquired with IVIS Spectrum In Vivo Imaging System. For in vivo inflammation experiments, female nu/nu mice were given an intraperitoneal (i.p.) injection of LPS (1mg in 1 mL saline) to induce peritonitis. After 4 h, the mice were anesthetized. Then the mice were i.p. injected with $PFOBT_{36}SeTBT_5$ Pdots (0.3 mg/mL 0.2 mL). As a control, unstimulated mouse, which were i.p. injected with saline not containing LPS, were also prepared. Fluorescence images were acquired 30 min after injection of $PFOBT_{36}SeTBT_5$ Pdots. Fluorescence image

analysess used the peritoneal cavity as region of interest. Ratiometric images were obtained by pixel-by-pixel calculation using Image J software.

Table S1. Comparison of recently reported probes for the sensing of ClO^-

Probe	Output signal	Sensing performance	application	comments
Small molecules:				
STP-HOCl[4]	Ratiometric I_{520nm}/I_{470nm}	0-150 μM, Excellent selectivity for ClO^-	Endogenous ClO^- imaging in HeLa cells and ClO^- treated living liver slice	First two-photon ratiometric HOCl fluorescent probe
CY-FPA[5]	"On-Off" NIR I_{774nm}	0.7 μM, Excellent selectivity for ClO^-	Evaluate the enzymatic MPO system, imaging of ClO^- pre-treated A549 cells	Colorimetric and NIR fluorescent dual functional probe, good cell permeability and low cytotoxicity
SO3H-APL[6]	Bioluminescence "Off-On"~I_{620nm}	ClO^-(0.032 μM), $ONOO^-$ (0.51 μM), ·OH(7.3 μM), H_2O_2(0.25 μM)	Bioluminescence imaging of exogenous and endogenous hROS in mice	Highly sensitive bioluminogenic probe that can detect physiological amounts of hROS clearly and non-invasively in deep tissues
Ru-Fc[7]	"Off-On" Red I_{626nm}	38.6 μM, Good selectivity for ClO^-	Imaging of exogenous ClO^- in MDA-MB-231 cells and live Daphnia magna	High sensitivity and selectivity, and good biocompatibility, lysosomal HOCl imaging reagent
HKOCl-3[8]	"Off-On" Green I_{527nm}	0.33 nM, ultra-selectivity for ClO^-	Endogenous ClO^- imaging in multiple cell types, live intact zebrafish embryos	ultra-selectivity, ultra-sensitivity and rapid turn-on fluorescent response
RSTPP[9]	"Off-On" Red I_{580nm}	9 nM, good selectivity for ClO^-	Fluorescence images of ClO^- in RAW264.7 cells during E. coli infection	Accurate mitochondrial-targeting ability, fast response, excellent selectivity and high sensitivity
MMSiR[10]	"Off-On", Far red to NIR I_{670nm}	0-5 μM, good selectivity for ClO^-	In vivo imaging of HOCl generation in a mouse peritonitis model	Far-red to NIR fluorescence probe, pH-independence, tolerance to autoxidation and photobleaching
FBS[11]	"Off-On" Green I_{523nm}	0-20 μM, good selectivity for ClO^-	Detection of DUOX-dependent HOCl induction in Drosophila gut system	High selectivity, can be used in neutral, acidic, and basic solutions
FHZ[12]	"Off-On" H_2O_2: I_{486nm} ClO^-: I_{520nm}	ClO^-: 0.5-200 μM H_2O_2: 10-1000 μM Good selectivity for ClO^-	Imaging of ·OH and HOCl spiked in HeLa cells, endogenous ·OH and HOCl in cellular mitochondria and zebrafish	Distinguishable ability in the coexistence of two ROS, rapid, sensitive and dynamic responses, high biocompatibility
CS2-7[13]	"Off-On" NIR $I_{746\ nm}$	0-70 μM, good selectivity for ClO^-	Endogenous ClO^- imaging in Raw 264.7 cells and in living mice	Novel NIR fluorescent TURN-ON sensor
Nanoprobe:				
C-dots-AuNC[14]	Ratiometric I_{455nm}/I_{565nm}	ClO^-, $ONOO^-$, ·OH (About 0.5 μM)	Endogenous ClO^- imaging in Raw 264.7 cells and local ear inflammation in mice	Simple and convenient fabrication process, ratiometric fluorescence with high contrast
DEFN[15]	Ratiometric I_{435nm}/I_{565nm}	·OH (0.03 μM), $ONOO^-$ (0.2 μM), ClO^- (0.5 μM)	Exogenous ClO^- imaging in HeLa cells, endogenous ClO^- imaging in Raw 264.7 cells	Ratiometric fluorescence with high contrast and accuracy, excellent biocompatibility, high intracellular delivery efficiency, superb stability
$Zn(DZ)_3$[16]	Ratiometric I_{544nm}/I_{659nm}	3 nM, good selectivity for ClO^-	Exogenous ClO- imaging in HeLa cells	High sensitivity, selectivity, rapid response, minimal background fluorescence
NanoDRONE[17]	Ratiometric I_{678nm}/I_{818nm}	$ONOO^-$, ClO^-, ·OH (About 10 nM)	Endogenous ClO^- imaging in Raw 264.7 cells, acute peritonitis mouse and bacterial infected mouse	High physiological stability, good biodistribution and long circulation half-life, and passive targeting to inflammatory regions, NIR fluorescent imaging
HA-UCNPs[18]	Ratiometric I_{540nm}/I_{654nm}	·OH (0.03 μM), ClO^- (0.02 μM), $ONOO^-$ (0.06 μM), O_2^- (0.1 μM)	In vitro imaging ROS in Raw 264.7 cells and in vivo imaging ROS in arthritic mice	High sensitivity towards both highly ROS and superoxide anion, colloidal stability and good biocompatibility

ThioRB-FITC-MSN[19]	Ratiometric I_{586nm}/I_{526nm}	0-80 μM, good selectivity for ClO^-	Exogenous ClO^- imaging in L929 cells	Ratiometric reporting of HOCl in lysosomes in cells, compatible with conventional flow cytometry
SiO_2-1@mSiO_2-2[20]	Ratiometric I_{598nm}/I_{500nm}	0-50 μM，good selectivity for ClO^-	Exogenous and endogenous ClO^- imaging in Raw 264.7 cells	Ratiometric and lifetime-based detection, distinguishable phosphorescence signals
$PFOBT_{36}SeTBT_5$ Pdots (this work)	Ratiometric I_{540nm}/I_{680nm}	0.5 μM, excellent selectivity for ClO^-	Exogenous ClO^- imaging in MCF-7 cells and mouse, endogenous ClO^- imaging in Raw 264.7 cells and acute peritonitis in mouse	Far-red to NIR ratiometric sensor with high contrast and accuracy, high photostability, high selectivity, rapid response, pH-independence

Table S2. Size and quantum yield (QY) characterizations of $PFOBT_{36}SeTBT_x$ Pdots.

	$PFOBT_{36}SeTBT_3$	$PFOBT_{36}SeTBT_5$	$PFOBT_{36}SeTBT_7$
size	22.83±1.086 nm	23.52±0.9815 nm	22.94±1.556 nm
QY (pure Pdots) (560-900 nm)	16.7	13.6	9.3
QY (pure Pdots) (490-560 nm)	0	0	0
QY (500 uM NaClO) (560-900 nm) ↓	8.6	7.3	4.9
QY (500 uM NaClO) (490-560 nm) ↑	0.7	0.5	0.4

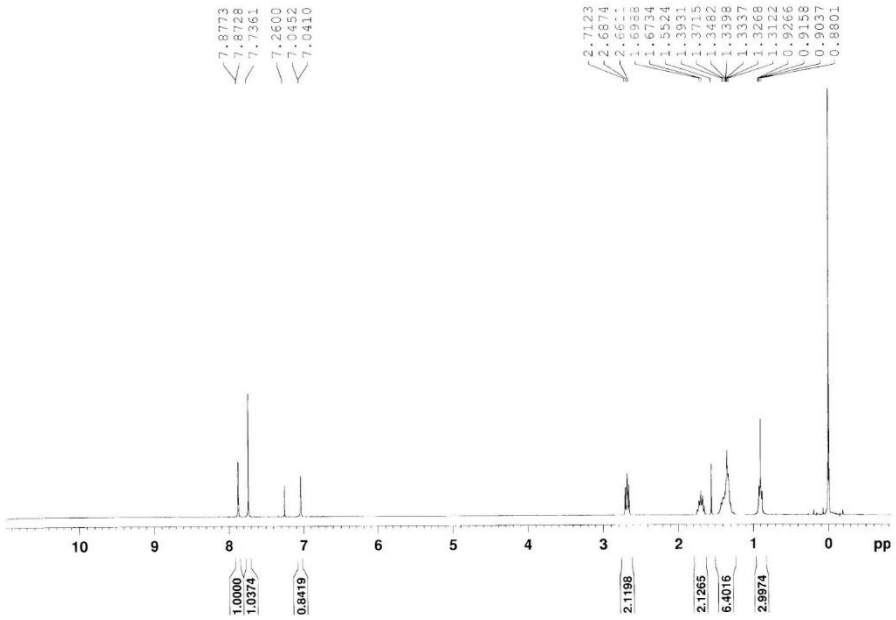

Figure S1. ^1H NMR of 4,7-bis(4-hexylthiophen-2-yl)benzo[c][1,2,5]selenadiazole.

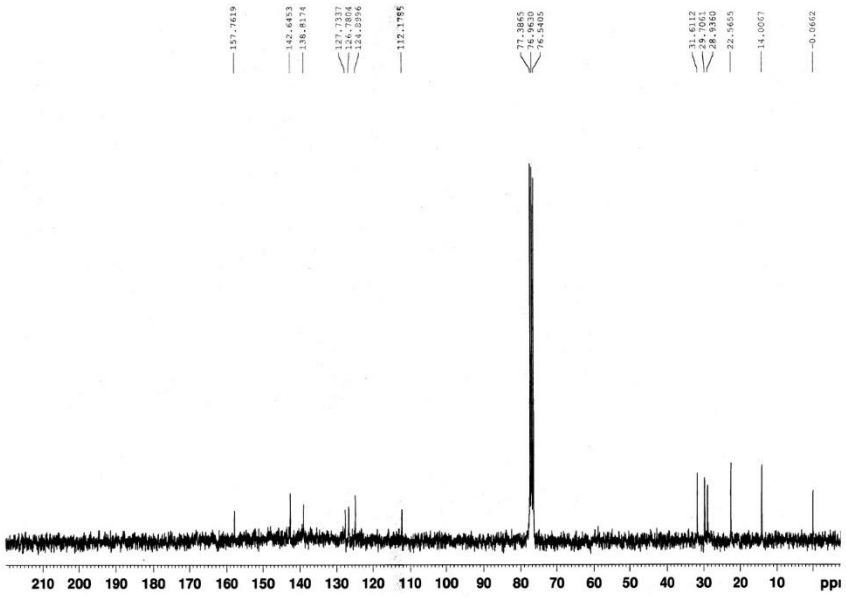

Figure S2. ^{13}C NMR of 4,7-bis(4-hexylthiophen-2-yl)benzo[c][1,2,5]selenadiazole.

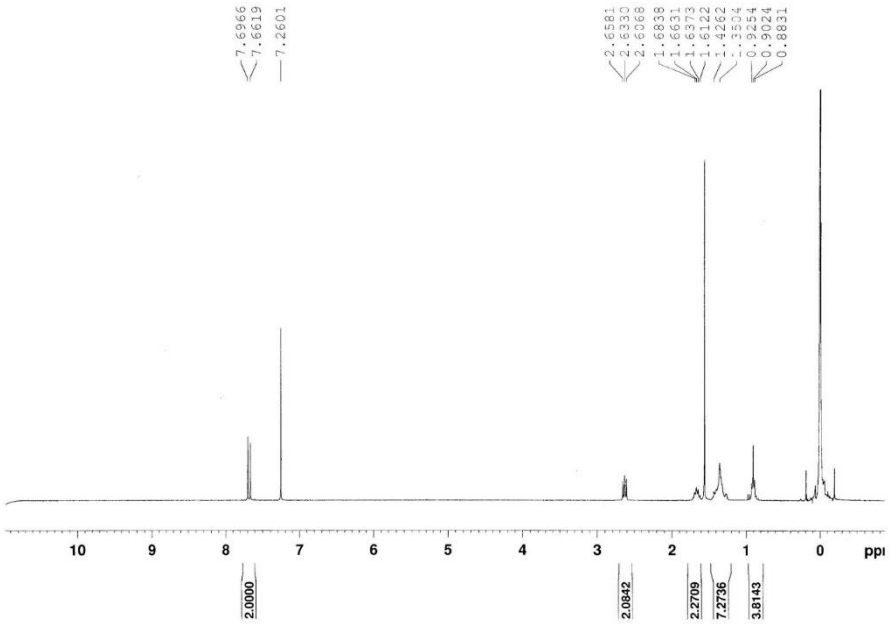

Figure S3. ^{1}H NMR of 4,7-bis(5-bromo-4-hexylthiophen-2-yl)benzo[c][1,2,5]selenadiazole.

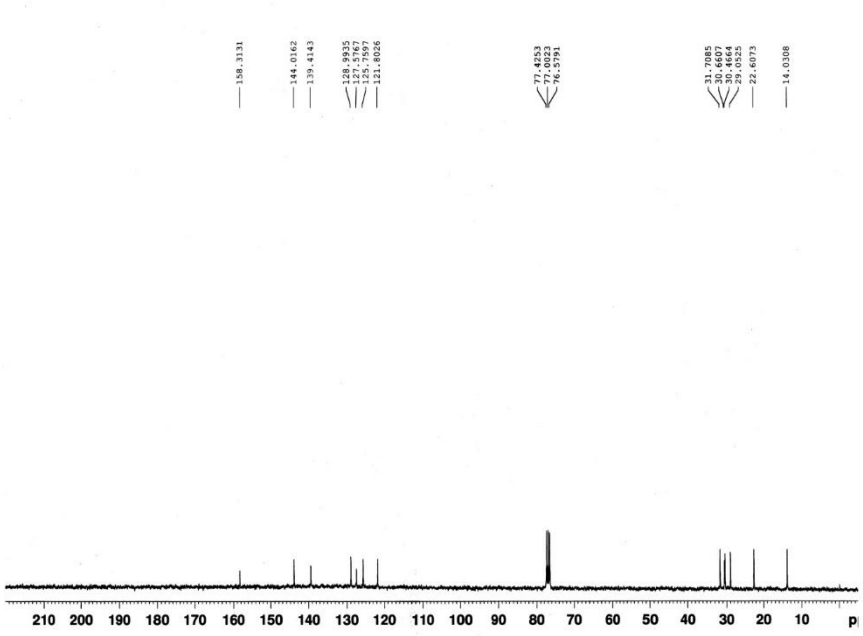

Figure S4. ^{13}C NMR of 4,7-bis(5-bromo-4-hexylthiophen-2-yl)benzo[c][1,2,5]selenadiazole.

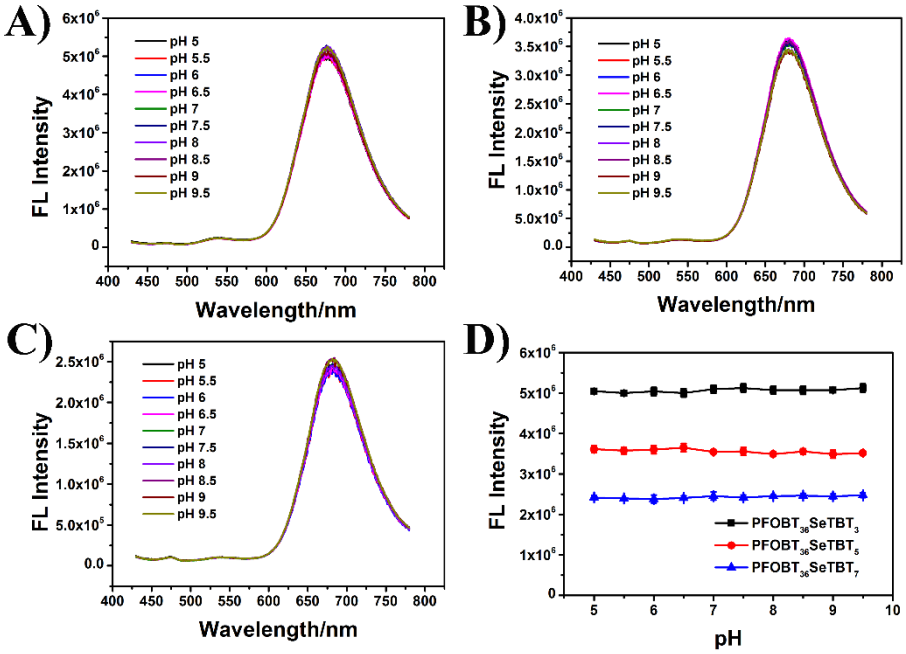

Figure S5. The pH stability of $PFOBT_{36}SeTBT_3$ (A), $PFOBT_{36}SeTBT_5$ (B), and $PFOBT_{36}SeTBT_7$ (C) Pdots. D) is the relationship between the fluorescence intensity and pH value in PBS solution.

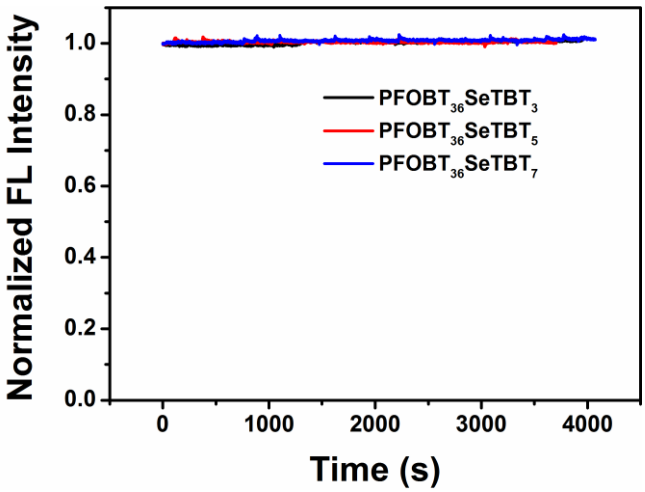

Figure S6. Photostability of the Pdots (normalized fluorescence intensity *vs.* time). All the spectra were obtained with the excitation wavelength of 405 nm and recorded the fluorescence intensity at the emission wavelength of 680 nm.

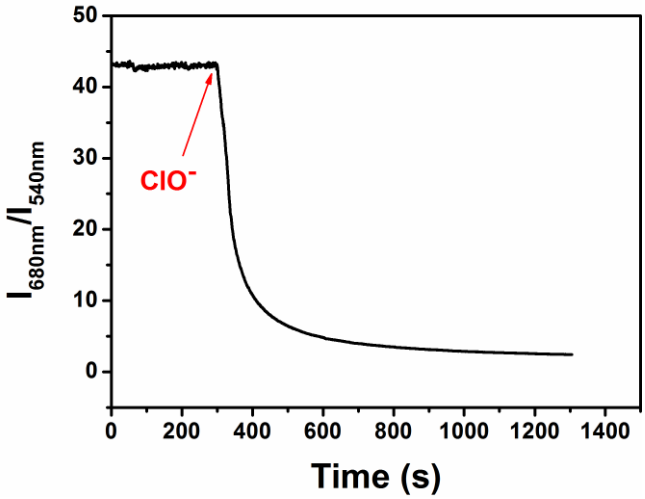

Figure S7. The fast response of $PFOBT_{36}SeTBT_5$ Pdots toward ClO^- detection. Time course of the fluorescence intensity ratio of 10 μg/mL $PFOBT_{36}SeTBT_5$ Pdots with 100 μM ClO^- in PBS (10 mM, pH 7.4).

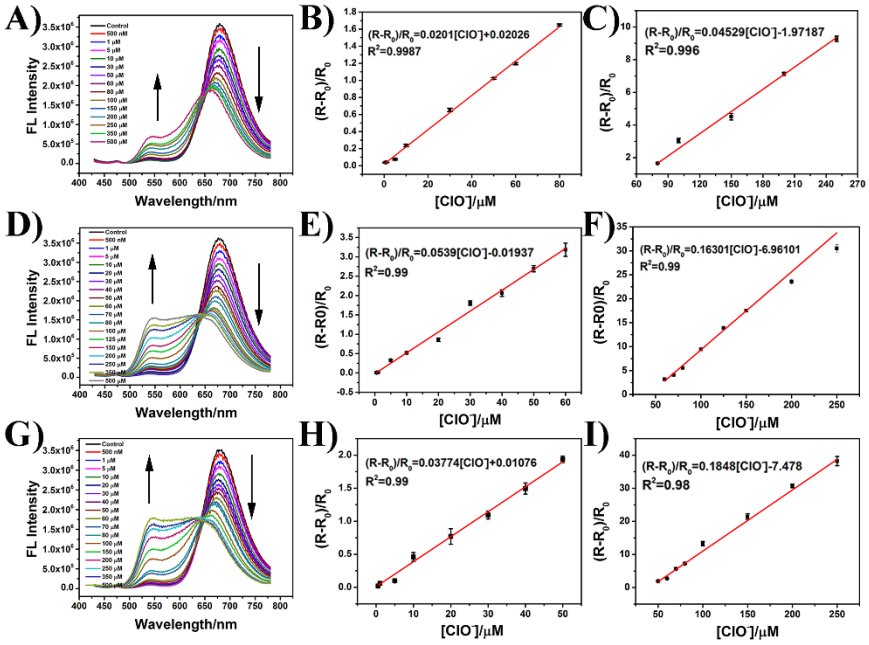

Figure S8. The sensing performance of $PFOBT_{36}SeTBT_5$ Pdots toward ClO^- in PBS solution with different pH values: pH 5 (A-C), pH 6 (D-F), pH 9 (G-I).

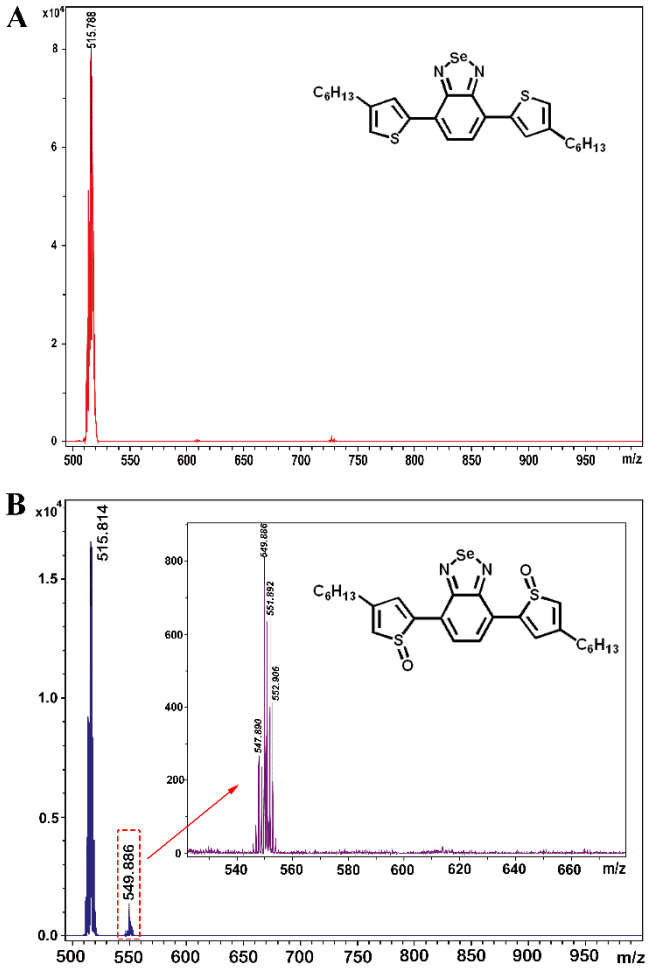

Figure S9. MALDI-TOF spectra of SeTBT before (A) and after (B) reaction with ClO^-.

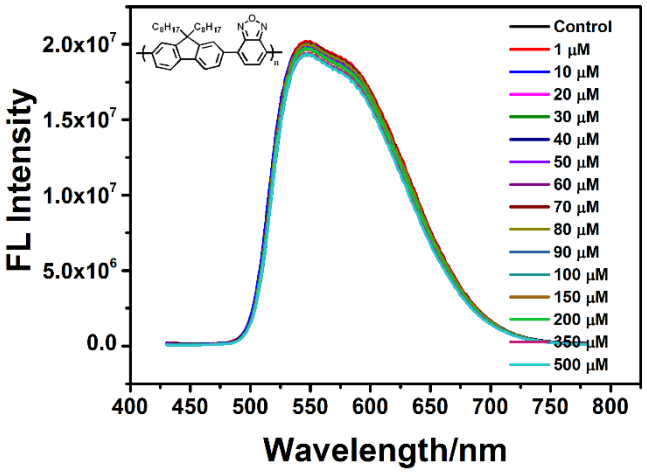

Figure S10. The fluorescence performance of PFOBT Pdots in the presence of different concentrations of ClO^- ions (inset: structure of PFOBT).

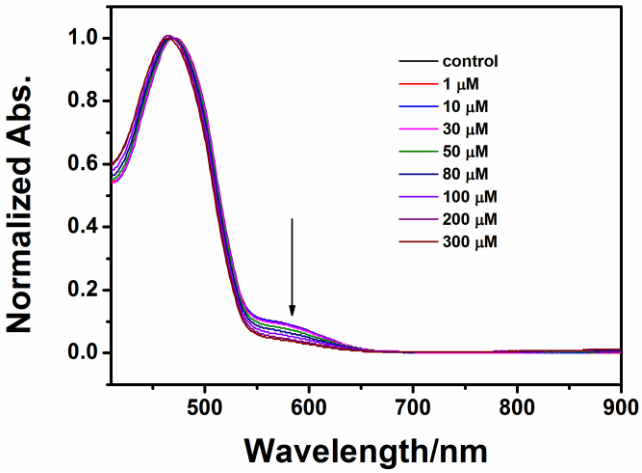

Figure S11. Normalized UV-vis spectra of $PFOBT_{36}SeTBT_5$ Pdots in the presence of different amounts of ClO^-.

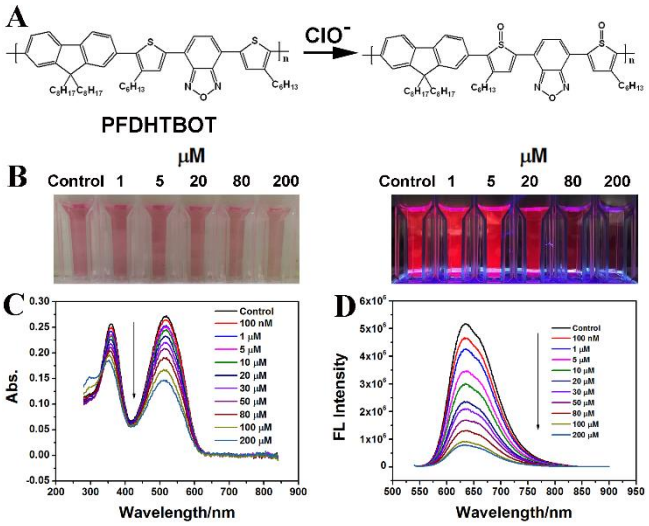

Figure S12. (A) Reaction mechanism of PFDHTBOT Pdots with ClO^-; (B) photographs of PFDHTBOT Pdots with the addition of ClO^- taken under normal laboratory lighting and illumination with a UV light at 365 nm; (C) UV-vis spectra of PFDHTBOT Pdots in the presence of different amount of ClO^-; (D) The fluorescence performance of PFDHTBOT Pdots in the presence of different concentration of ClO^- ions, ex=520 nm. All the measurements were performed in 10 mM PBS solution (pH 7.4).

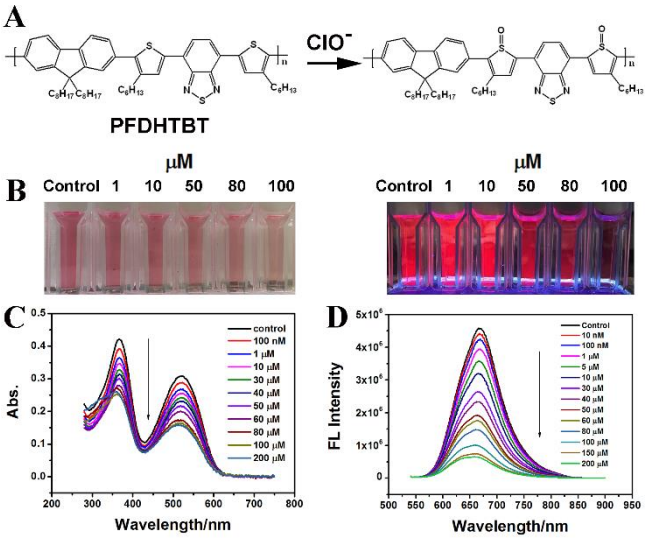

Figure S13. (A) Reaction mechanism of PFDHTBT Pdots toward ClO^-; (B) photographs of PFDHTBT Pdots with the addition of ClO^- taken under normal laboratory lighting and illumination with a UV light at 365 nm; (C) UV-vis spectra of PFDHTBT Pdots in the presence of different amount of ClO^-; (D) The fluorescence performance of PFDHTBT Pdots in the presence of different concentration of ClO^- ions, ex=520 nm. All the measurements were performed in 10 mM PBS solution (pH 7.4).

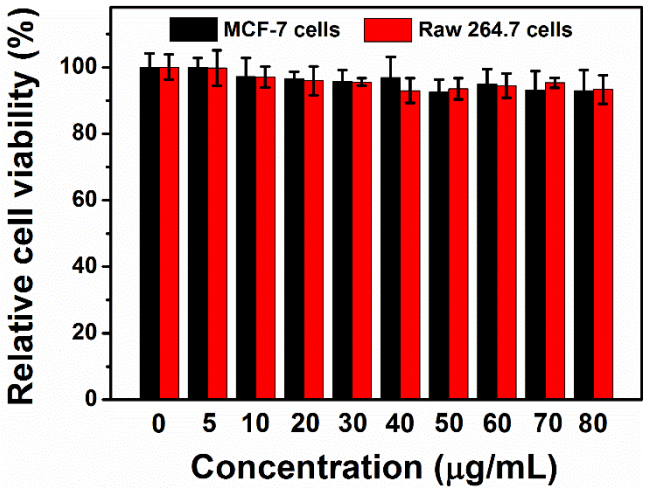

Figure S14. MTT characterization of the $PFOBT_{36}SeTBT_5$ Pdots; from left to right: control; 5 μg/mL; 10 μg/mL; 20 μg/mL; 30 μg/mL; 40 μg/mL; 50 μg/mL; 60 μg/mL; 70 μg/mL; 80 μg/mL.

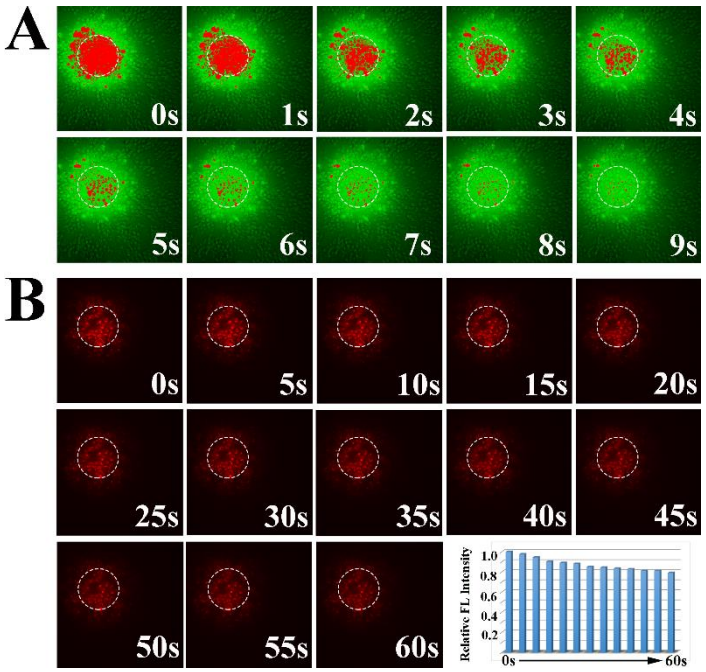

Figure S15. Test of photostability. Dynamic fluorescence images were recorded by time-sequential scanning of MCF-7 cells incubated with FITC dye (A) and PFOBT$_{36}$SeTBT$_5$ Pdots (B).

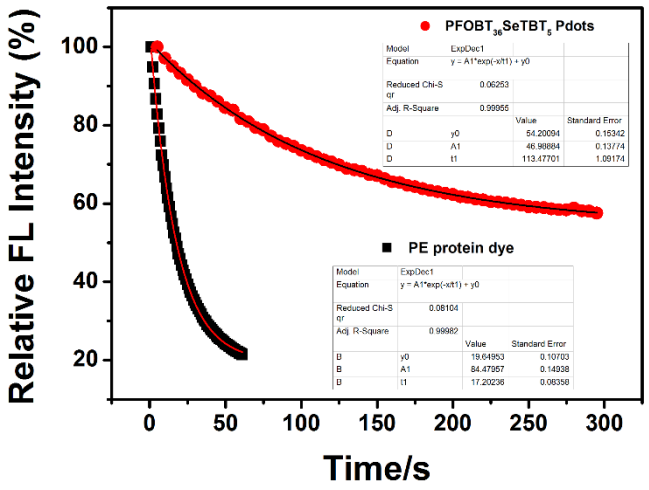

Figure S16. Comparison of the fluorescence decay curves of PFOBT$_{36}$SeTBT$_5$ Pdots and PE protein dye upon continuous laser irradiation.

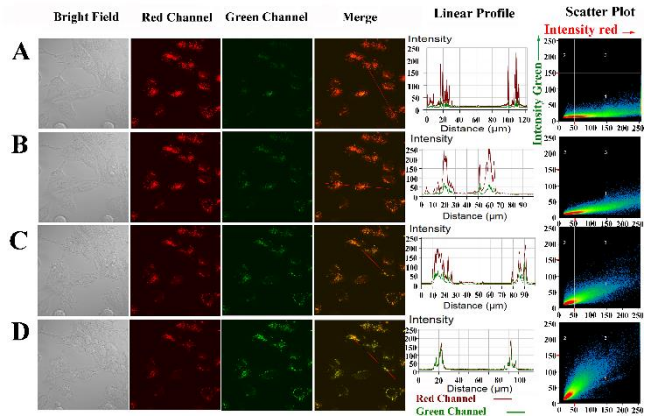

Figure S17. Time-dependent confocal fluorescence imaging of exogenous ClO^- in MCF-7 cells. $PFOBT_{36}SeTBT_5$-Pdot-loaded cells were treated with 50 μM NaClO; confocal fluorescence images were recorded at different time points: (A) 0, (B) 5, (C) 10, and (D) 15 min. Images were acquired by using 405-nm excitation and fluorescence emission windows of green channel (530-600nm) and red channel (>650 nm), respectively.

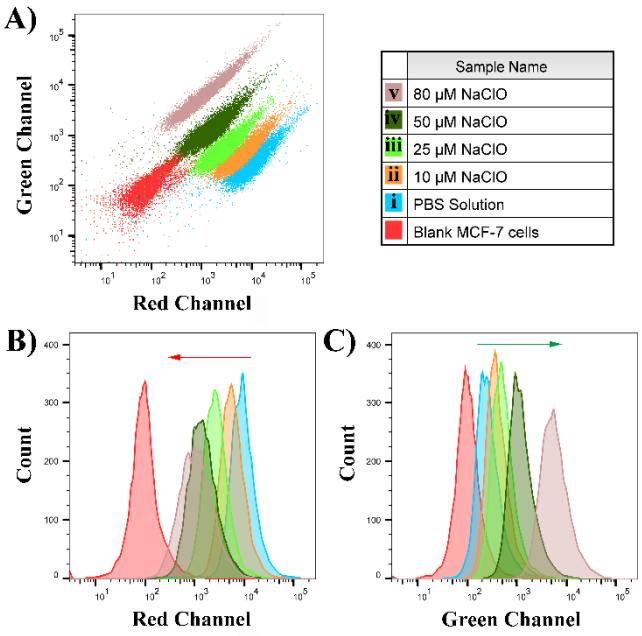

Figure S18. Flow cytometric analysis of Pdot nanosensor in MCF-7 cells with $PFOBT_{36}SeTBT_5$-Pdot under single wavelength excitation (ex: 405 nm). Dose-dependent fluorescent responses in MCF-7 cells treated with different levels of NaOCl were indicated. (A) Plot of two fluorescence channels; Histogram analysis of Red Channel (B) and Green Channel (C). MCF-7 cells first incubated with $PFOBT_{36}SeTBT_5$ Pdots (10 μg/mL) overnight at 37 °C and then incubated with different concentrations of NaClO for 30 min; (i) PBS solution; (ii) 10 μM NaClO; (iii) 25 μM NaClO; (iv) 50 μM NaClO; (v) 80 μM NaClO. The fluorescence of Red Channel was collected in the BV711 channel (685–760 nm) while that of the Green Channel was collected in the BV 500 channel (505–575 nm).

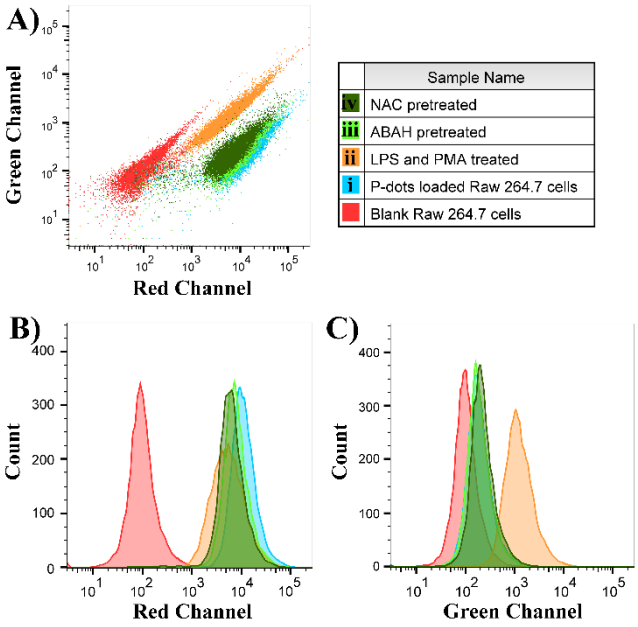

Figure S19. Detection of endogenous HOCl in flow cytometry with Pdot nanosensor. RAW264.7 cells were co-incubated with $PFOBT_{36}SeTBT_5$-Pdots (10 μg/mL, 4h) before analysis by flow cytometry: (i) nontreated cells; (ii) cells successively treated with LPS (4h) and PMA (0.5h); (iii) cells pretreated with ABAH 2h before treated with LPS (4h) and PMA (0.5h), followed with ABAH for 1 h; and (iv) cells pretreated with NAC 2h before treated with LPS (4h) and PMA (0.5h), followed with NAC for 1 h. [LPS]= 1 μg/mL; [PMA]= 5 μg/mL; [NAC]= 1 mM; [ABAH]= 1 mM. The fluorescence of Red Channel was collected in the BV711 channel (685–760 nm) while that of the Green Channel was collected in the BV 500 Channel (505–575 nm).

References:

(1) Chen, C.-P.; Huang, Y.-C.; Liou, S.-Y.; Wu, P.-J.; Kuo, S.-Y.; Chan, Y.-H. *ACS Appl. Mater. Interfaces* **2014**, *6*, 21585.

(2) Kuo, C.-T.; Thompson, A. M.; Gallina, M. E.; Ye, F.; Johnson, E. S.; Sun, W.; Zhao, M.; Yu, J.; Wu, I. C.; Fujimoto, B.; DuFort, C. C.; Carlson, M. A.; Hingorani, S. R.; Paguirigan, A. L.; Radich, J. P.; Chiu, D. T. *Nat. Commun.* **2016**, *7*, 11468.

(3) Sun, W.; Yu, J.; Deng, R.; Rong, Y.; Fujimoto, B.; Wu, C.; Zhang, H.; Chiu, D. T. *Angew. Chem. Int. Ed.* **2013**, *52*, 11294.

(4) Chen, H.; Shang, H.; Liu, Y.; Guo, R.; Lin, W. *Adv. Funct. Mater.* **2016**, *26*, 8128.

(5) Sun, M.; Yu, H.; Zhu, H.; Ma, F.; Zhang, S.; Huang, D.; Wang, S. *Anal. Chem.* **2014**, *86*, 671.

(6) Kojima, R.; Takakura, H.; Kamiya, M.; Kobayashi, E.; Komatsu, T.; Ueno, T.; Terai, T.; Hanaoka, K.; Nagano, T.; Urano, Y. *Angew. Chem. Int. Ed.* **2015**, *127*, 14981.

(7) Cao, L.; Zhang, R.; Zhang, W.; Du, Z.; Liu, C.; Ye, Z.; Song, B.; Yuan, J. *Biomaterials* **2015**, *68*, 21.

(8) Hu, J. J.; Wong, N.-K.; Lu, M.-Y.; Chen, X.; Ye, S.; Zhao, A. Q.; Gao, P.; Kao, R. Y.-T.; Shen, J.; Yang, D. *Chem. Sci.* **2016**, *7*, 2094.

(9) Zhou, J.; Li, L.; Shi, W.; Gao, X.; Li, X.; Ma, H. *Chem. Sci.* **2015**, *6*, 4884.

(10) Koide, Y.; Urano, Y.; Hanaoka, K.; Terai, T.; Nagano, T. *J. Am. Chem. Soc.* **2011**, *133*, 5680.

(11) Xu, Q.; Lee, K.-A.; Lee, S.; Lee, K. M.; Lee, W.-J.; Yoon, J. *J. Am. Chem. Soc.* **2013**, *135*, 9944.

(12) Zhang, R.; Zhao, J.; Han, G.; Liu, Z.; Liu, C.; Zhang, C.; Liu, B.; Jiang, C.; Liu, R.; Zhao, T.; Han, M.-Y.; Zhang, Z. *J. Am. Chem. Soc.* **2016**, *138*, 3769.

(13) Yuan, L.; Lin, W.; Yang, Y.; Chen, H. *J. Am. Chem. Soc.* **2012**, *134*, 1200.

(14) Ju, E.; Liu, Z.; Du, Y.; Tao, Y.; Ren, J.; Qu, X. *ACS Nano* **2014**, *8*, 6014.

(15) Chen, T.; Hu, Y.; Cen, Y.; Chu, X.; Lu, Y. *J. Am. Chem. Soc.* **2013**, *135*, 11595.

(16) Mei, Q.; Deng, W.; Yisibashaer, W.; Jing, H.; Du, G.; Wu, M.; Li, B. N.; Zhang, Y. *Small* **2015**, *11*, 4568.

(17) Pu, K.; Shuhendler, A. J.; Rao, J. *Angew. Chem. Int. Ed.* **2013**, *52*, 10325.

(18) Chen, Z.; Liu, Z.; Li, Z.; Ju, E.; Gao, N.; Zhou, L.; Ren, J.; Qu, X. *Biomaterials* **2015**, *39*, 15.

(19) Wu, X.; Li, Z.; Yang, L.; Han, J.; Han, S. *Chem. Sci.* **2013**, *4*, 460.

(20) Zhang, K. Y.; Zhang, J.; Liu, Y.; Liu, S.; Zhang, P.; Zhao, Q.; Tang, Y.; Huang, W. *Chem. Sci.* **2015**, *6*, 301.